LARGE REFLECTOR ANTENNA PROFILE MEASUREMENTS BY PHASE RETRIEVAL TECHNIQUES: AN ARRAY PROCESSING APPROACH

Juan E. Garrido-Arenas[1], José M. Páez-Borrallo[2], Alberto Barcia-Cancio[1]

[1] Centro Astronómico de Yebes, I.G.N., Apdo. 148, 19080 Guadalajara, SPAIN
[2] Dpto. S.S.R., E.T.S.I. Telecomunicación, Universidad Politécnica de Madrid, Ciudad Universitaria, 28040 Madrid, SPAIN

ABSTRACT

Determination of the surface quality of large reflector antennas by direct methods like tape-theodolite has been revealed as not accurate enough for millimeter-wave operation. Indirect methods like holographic ones have been widely used. They are based on the Fourier Transform (FT) relationship between the far-field pattern and the field distribution in the aperture, whose phase can be used to obtain the map of axial deformations of the paraboloid by simple ray tracing.

Measurement of the pattern phase requires a second antenna-receiver system and becomes difficult for high frequencies, so the possibility of recovering the aperture field from only-amplitude (or intensity) measurements of its FT (the pattern) has been studied and applied in radio telescope measurements. We present a discrete model for the aperture that enables us to approach this problem from an array processing point of view.

1. APERTURE DISCRETE MODEL

Both, pattern measurement and data processing imply digital processing, with the typical requirements and limitations: sampling interval, size of the data window, etc. In our case, we have the advantage that the function has a finite support in the aperture domain, which is a kind of bandlimitedness. A first step in the modelization is the establishment of a discrete model valid for the representation of the continuous aperture, so that the aperture and its radiated field are well represented by an equivalent array.

We can start by considering the expression relating the radiation integral $\boldsymbol{P}$, a function proportional to the far-field pattern radiated by a finite continuous aperture, with the complex field in the aperture, $\boldsymbol{E}_a$:

$$\boldsymbol{P}(\boldsymbol{r}) = \int_{S_a} \boldsymbol{E}_a(\boldsymbol{r}') \ \exp\left(jk\boldsymbol{r}'\cdot\boldsymbol{r}\right) \ ds' \qquad (1)$$

where S_a is the aperture extent, $k = 2\pi/\lambda$, $\boldsymbol{r}'$ the position vector of the element of surface to be integrated, ds', and $\boldsymbol{r}$ the unit vector in the observing direction.

If we consider just one component of the field polarization (the other can be treated in parallel, if it exists), for example, linear in the y direction, and the aperture is located in the xy plane ($z = 0$), we have the following expression:

$$P_y(u,v) = \int_{S_a} E_{ay}(x',y')\exp\left(j2\pi\left(x'u + y'v\right)\right)dx'dy' \qquad (2)$$

where u=sinθcosφ and v=sinθsinφ are the director cosines of the observing direction over the xy plane and x',y' (in wavelengths) is the position vector of the surface element to be integrated, dx',dy'. (2) is a FT type expression. $P_y(u,v)$ or $E_{ay}(x',y')$ can be sampled over a cartesian grid, yielding:

$$P_y\left(u_p, v_q\right) = \sum_{m=0}^{N-1}\sum_{n=0}^{N-1} E_{ay}\left(x'_m, y'_n\right)\exp\left(j2\pi d\left(mu_p + nv_q\right)\right)$$
$$m,n,p,q = 0,1,\ldots,N\text{-}1 \qquad (3)$$

where d is the sampling interval in the aperture domain, in wavelengths.

Since (3) provides the radiated field in the points of interest, the continuous aperture can be replaced by an equivalent array of isotropic elements placed over the planar grid, with weights given by $E_{ay}(x'_m,y'_n)$. On the other hand, the two dimensional Discrete Fourier Transform (DFT) of the array weights can be calculated as:

$$P(p,q) = \sum_{m=0}^{N-1}\sum_{n=0}^{N-1} E(m,n)\exp\left(j(2\pi\ /\ N)(mp + nq)\right)$$
$$m,n,p,q = 0,1,\ldots,N\text{-}1 \qquad (4)$$

this discrete finite function has period N in both p and q variables, and is equivalent to (3) within one period if the following equalities hold:

$$u_p = \frac{p}{Nd} \quad ; \quad v_q = \frac{q}{Nd} \qquad (5)$$

Then, the DFT of the array weights is equivalent to the sampled array pattern with an interval $1/Nd=1/D$, where D is the array dimension in the direction of one of the axes, expressed in wavelengths.

The physical meaning of $P(p,q)$ will depend on the values selected for N and d. If d=1/2, the visibility range (VR) coincides with one period of $P(p,q)$, if d<1/2, VR is smaller than a period

0-7803-2431-5/95 $4.00

of $P(p,q)$ and if $d>1/2$, the usual situation, VR has more than one period of $P(p,q)$ which, for a real array means that the grating lobes will appear. In our case we shall consider the measured data window to be much smaller than a hemisphere, being neglected the values outside the window.

2. PHASE RETRIEVAL. MISELL ALGORITHM

Phase retrieval algorithms are needed, in general, when the operating frequencies are high enough to make the phase measurements not practical. The two-dimensional nature of the problem is an advantage, because the zero measure of the set of reducible polynomials in two variables (to which Z-Transforms of the field functions belong), guarantees the uniqueness of the solution except for trivial ambiguities [1].

2.1. Iterative algorithms

A general phase retrieval scheme is depicted in figure 1. Its main elements are: a coupled direct-inverse FT, two projections (one in each domain) to force *a priori* physical and measurement constraints and a feasible initial guess of the aperture field. An underlying cost function of the form $E_i=(|P_i|-|P|)^2$ is minimised and can be evaluated at each iteration as an indication of convergence [2]. P_i is the resulting pattern at iteration i and $|P|$ is the measured modulus. However, minimisation of cost functions of the form:

$$E_i = \left(|P_i|^q - |P|^q\right)^r \qquad (6)$$

is a natural generalisation to be further investigated in this application, selecting optimum q and r. In this direction, Isernia et al. [3] have shown the better behaviour of $q=r=2$ instead of $q=1$, $r=2$.

The Misell algorithm, developed in electron microscopy, is one of the most widely used in radiotelescope measurements [4]. This algorithm needs a starting aperture field with random phase and ideal amplitude (the nominal for the antenna). It takes as inputs two measured radiation patterns with different focus settings, which correspond to the measurement constraints. The physical constraints for this application are the aperture support and the defocus amounts applied to measure the patterns. This way, each iteration comprises two passings trough the loop of figure 1, applying the corresponding measured pattern to the current defocus.

2.2. Results from simulations

We present here results of a simulation representing a typical situation in telescope measurements. The antenna is a Cassegrain system (main reflector and subreflector which causes a central blocking). *D/f* (diameter over focal length ratio) is 0.3. Two defocussed maps with $+1\lambda$ and -1λ axial displacement of the secondary are generated over a 64x64 grid, to be taken as inputs to the algorithm. Gaussian noise is added to have a signal to noise ratio of 60 dB. The sampling interval is 0.8 times the critical Nyquist interval, in order to avoid aliasing in the aperture domain. The starting amplitude follows a gaussian profile with a -8 dB taper. 50 iterations have been performed and the resulting phases, in radians, are shown in figure 2.

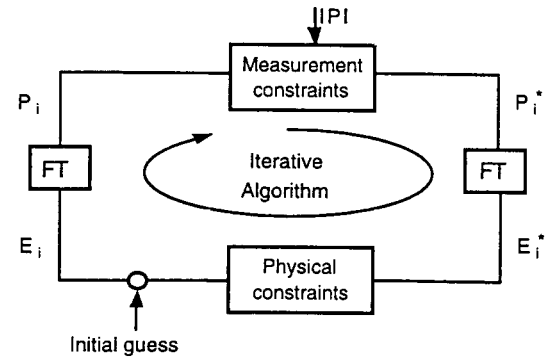

Figure 1. Phase retrieval block diagram

Note that, despite the high level of illumination at the edge (which can be selected by a lens in front of the feed), the phases are more noisy near this area than towards the center.

Figure 2 a) shows the retrieved aperture phase for an ideal antenna (constant phase across the aperture), with an rms of 4.2° due to the noise in the "measurement", as compared with the ideal value of zero degrees. In figure 2 b), the antenna has a phase distortion with sinusoidal shape in the y direction, 1 period across the aperture and with a 30° peak which would produce a rms phase of 21.2° which agrees very well with the rms phase of 23.1° of the retrieved solution. This is a realistic and simple approximation to the distortions caused by gravitational deformations.

2.3. Results from real data

In figure 3 we present results for the 14 m radio telescope at Yebes (Spain), obtained after averaging three independent results from Misell algorithm, taking different input patterns measured using the 49.49 GHz beacon for propagation studies of the geostationary satellite Italsat. Horizontal and vertical scales are in meters, amplitude contours are 5% to 95% in 10% intervals. An outline on the component panels is shown together with the phase map. The antenna is Cassegrain, with a 13.72 m diameter primary, a 1.085 m secondary, a *D/f* of 0.37 and, because we measure at the top end of the frequency band of our 7 mm receiver, the illumination taper is -16 dB. Sampling interval is 72" (0.79 that of Nyquist).

The pattern pairs used for the three results have the defocus values, $(+1.6,-0.6)\lambda$, $(+0.8,-0.6)\lambda$ and $(0.0,+1.6)\lambda$. A zero padding is made on the 32x32 pixel measured patterns to get 64x64 elements results. A circular window of 12 pixel radius was applied to all radiation patterns in order to remove noise and radome effects. The size of the window was selected as a compromise between the removal of these error sources and the loss of resolution.

Each independent result was obtained after averaging 5 repetitions of the Misell algorithm on each pattern pair, with different random initial phases, 500 iterations each repetition. Then, the three independent results were averaged again. The first averaging step tends to reduce noise in the following two ways: averaging is equivalent to low pass filtering, and the "locked" individual results tend to be randomly distributed

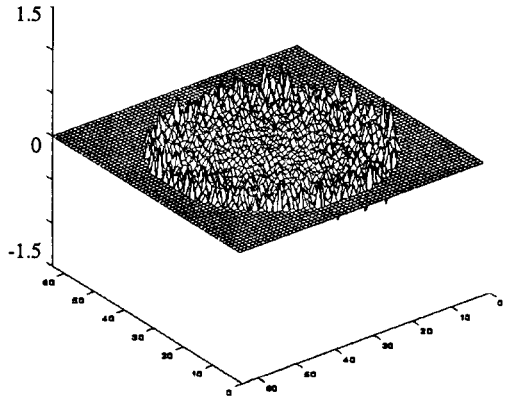

a)

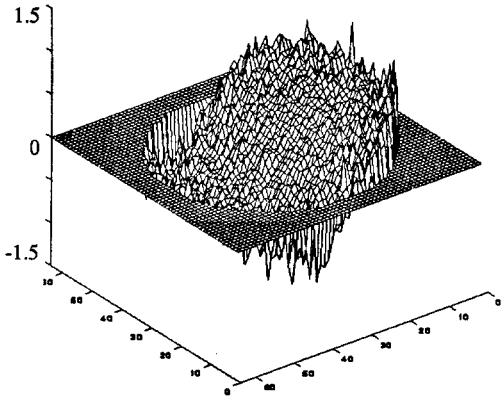

b)

Figure 2. Resulting phases of simulations:
a) *Perfect antenna,* b) *Distorted antenna*

around the global minimum of the cost function [4]. The second step, in addition, forces different measurement constraints on the algorithm and tends to eliminate possible effects caused by the particular characteristics of a single set of constraints.

The phase solution is fairly good in all zones where the amplitude is high enough (otherwise the phases are random, not significative) and very similar in all the individual results, so we can conclude that the large scale errors (> 2 m) are recovered. It is important to note that the circular windowing improves the results, making them less noisy, of better visual quality and more reliable: we can see now the "hole" corresponding to the secondary blocking, absent when the window was not applied

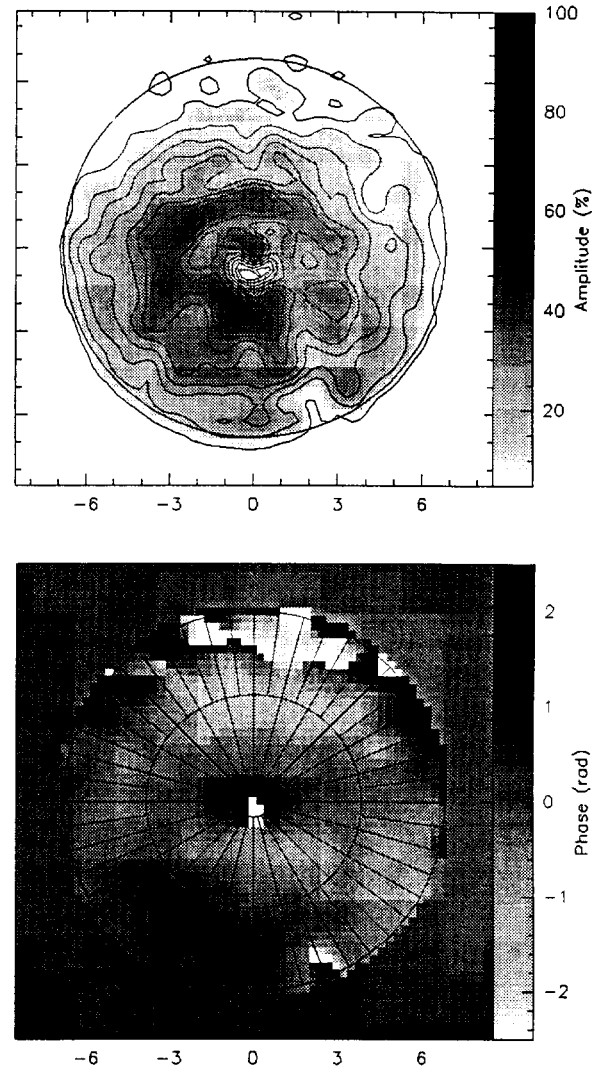

Figure 3. Results for the Yebes 14 m antenna

(the bad pointing of the feed can cause the slight offset downwards from the center, see figure 3). The phase depression observed at the lower right edge of the reflector is related to a panel tilt forced on the surface for qualitative testing of the algorithm.

Final rms phase is 37° (rms surface axial deviation of 313 μm), which would cause an efficiency multiplicative factor of 65% at 49 GHz assuming a random distribution of the errors, but in fact, as their shape reveals a systematic deformation (gravitational), the factor is worse, around 50% at 43 GHz, as can be deduced from efficiency measurements made on planets.

3. ARRAY PROCESSING APPROACH

As stated in point 1, we have an array model for our continuous aperture, so we can use the powerful tools of array processing to solve the posed problem: find the array which matches the pattern or patterns at the measured points plus all the possible

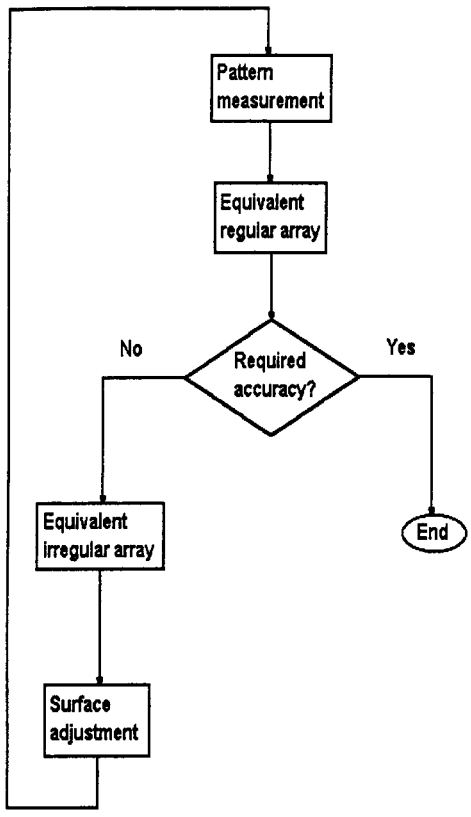

Figure 4. Procedure block diagram

constraints considered. This can be stated as a beamforming problem in which phase solution for the elements is capital, arising the difficulties from the lack of pattern phase information.

3.1. Further considerations

Due to the circular shape and polar arrangement of the panels of most reflector antennas and the improvement reached with circular masking on real data, performance of an equivalent polar array is being analysed. Despite the fact that it is easier to measure the pattern around the main beam in a cartesian grid, due to the tracking system of most large antennas, we can interpolate the measured data to have a polar grid and work with a polar-based algorithm [5]. The loss of computational efficiency is not determinant because we are processing off-line. This problem would be serious in a hypothetical active system which continuously measured and adjusted the surface of the antenna.

A further step is to find an array with ideal elements (nominal amplitude of the antenna for each position and uniform phase), but with three dimensional displacements from the original point in the grid calculated to match the previous regular array. In this way we will have a geometrical indication of the deviations that cause the errors of the wave front in the aperture using array techniques instead of the previously used ray tracing. The coarray concept [6] is useful to develop this step.

3.2. Measurement-adjustment procedure

The final goal of this study is to settle a measurement-adjustment procedure with the following steps:

1) Measurement of the amplitude or power radiation patterns on a prescribed grid.

2) Calculation of the equivalent array on the corresponding regular grid, for the real antenna.

3) Determination of the positional modifications needed so as to have an equivalent array of ideal elements.

4) Calculation and application of the correction to the real antenna.

The procedure is iterative, returnig to point 1) to check the adjustment made in 4) and proceeding until the required quality is reached.

A block diagram of this procedure is shown in figure 4. Implementation of step 4) from 3) implies a univocal matching between the resulting element displacements and the geometrical corrections on the antenna, which can be performed in two ways: by readjusting the z position of the screws supporting the individual primary reflector panels or by reshaping the secondary.

ACKNOWLEDGEMENT

We thank to D. Morris for his unvaluable help and for the software supplied to process the Yebes antenna data.

This work has been partially supported by Spanish DGICYT under grant PB 93-48.

REFERENCES

[1] M.H. Hayes, "The Reconstruction of a Multidimensional Sequence from the Phase or Magnitude of its Fourier Transform", IEEE Trans. on Acoustics, Speech and Signal Processing, Vol. ASSP-30, No. 2, pp. 140-154, Apr. 1982

[2] J.R. Fienup, "Phase retrieval algorithms: a comparison", Applied Optics, Vol. 21, No. 15, pp. 2758-2769, 1 Aug. 1982

[3] T. Isernia, G. Leone, R. Pierri, "Phaseless near field techniques: uniqueness conditions and attainment of the solution", Journal of Electromagnetic Waves and Applications, Vol. 8, No. 7, pp. 889-908, 1994

[4] D. Morris, "Phase Retrieval in the Radio Holography of Reflector Antennas and Radio Telescopes", IEEE Trans. on Antennas and Propagation, Vol. AP-33, No. 7, pp. 749-755, Jul. 1985

[5] W.H. Fang, A.E. Yagle, "Two-Dimensional Linear Prediction and Spectral Estimation on a Polar Raster", IEEE Trans. on Signal Processing, Vol. 42, No. 3, pp. 628-641, Mar. 1994

[6] R.T. Hoctor, S.A. Kassam, "The Unifying Role of the Coarray in Aperture Synthesis for Coherent and Incoherent Imaging", Proc. of the IEEE, Vol. 78, No. 4, pp. 735-752, Apr. 1990